ZHOU Zhibo
WANG Yan
XU Jiawei
LI Bo

Preliminary experimental scheme for two–dimensional heat and moisture transfer in porous building materials

To investigate the two-dimensional heat and moisture transfer behaviour in building porous materials and analyze the influence of edge sealing conditions on their thermophysical and hygric properties, this study proposes a new experimental scheme. Three typical construction materials — rock wool board, extruded polystyrene (XPS) board, and foam concrete — were selected as test specimens. By monitoring real-time temperature and humidity variations inside and outside the experimental setup, the coupled heat and moisture transfer characteristics of different materials were examined. The results demonstrate that materials with high water vapour resistance and effective air tightness significantly enhance thermal and hygric stability. Furthermore, for loosely structured porous materials, moisture loss through lateral edges leads to non-uniform humidity distribution within the material. Based on experimental data, this study quantitatively determined the water vapour permeability coefficients of the three materials and elucidated the underlying mechanisms. The proposed experimental method establishes a new approach for measuring 2D coupled heat and moisture transfer in building materials, providing a scientific framework for studying heat and moisture transport mechanisms in architectural applications.
Keywords: *porous materials, heat and moisture transfer, experimental protocol*

INTRODUCTION

Against the backdrop of increasingly prominent climate change and environmental pollution, building energy efficiency has become a critical issue for governments worldwide. As the largest energy consumer, China faces significant challenges in improving building energy performance. Porous building materials, characterized by their unique solid-gas two-phase structure, are widely used in building envelopes, insulation systems, and decorative materials. The pore characteristics and physical properties of these materials play a decisive role in heat and moisture transfer, impacting not only the durability of buildings but also indoor thermal and hygric environments and human comfort [1]. Consequently, extensive research has been conducted on the heat and moisture transfer properties of porous building materials, aiming to optimize material performance for reduced energy consumption and improved indoor environmental quality. In this context, developing convenient and reliable experimental methods for heat and moisture transfer is of great theoretical and practical value for revealing the underlying mechanisms of heat and moisture migration in porous building materials [2].

Domestic and international standards for testing the heat and moisture transfer performance of porous building materials have formed a relatively comprehensive system, gradually evolving toward dynamic, intelligent, and micro-scale characterization. In China, the cup method (GB/T 17146–2019) serves as the core testing technique, supplemented by the desiccant and wet-dish methods for measuring water vapour transmission rates. Recently, the China Academy of Building Research developed a dynamic climate chamber method to simulate temperature and humidity cycles for comprehensive performance evaluation [3, 4] Internationally, ISO 12572 employs the dry-wet cup method to determine moisture permeability coefficients[1], ASTM E96 is suitable for grading tests of thin-film materials[2], and the Nordic NT BUILD 428 quantifies liquid water transport coefficients in cement-based materials through capillary absorption tests.

Technological innovations in this field include the use of scanning electron microscopy (ESEM) by Academician Liu Jiaping to reveal the hydration kinetics and microstructural evolution of ultra-high-performance cement-based composites under low to moderate curing temperatures [5]. Professor Meng Qinglin developed a thermal-hygric climate wind tunnel test bench combined with infrared thermography and optical fiber sensing for dynamic monitoring of moisture resistance in building envelopes [6]. The Fraunhofer Institute for Building Physics (IBP) employs high-precision climate chambers with multi-field coupling control and dynamic climate simulation to address gaps in traditional testing methods for complex environmental conditions.

Current cutting-edge research integrates multidisciplinary technologies, such as CT scanning and numerical simulation for analyzing the influence of pore structures on heat and moisture transfer in aerogels [7], infrared thermography and spectral analysis (e.g., FTIR) for real-time monitoring of surface temperature and humidity distributions in smart materials, AI image recognition and infrared thermography for non-destructive testing and real-time monitoring of material defects [8], and digital twins combined with reinforcement learning (e.g., LSTM

[1] ISO 12571:2013. Hygrothermal performance of building materials and products — Determination of hygroscopic sorption properties [S]. 2013.

[2] ASTM C1498-04a. Standard Test Method for Hygroscopic Sorption Isotherms of Building Materials [S]. 2016.



ZHOU Zhibo,
Ph.D., Lecturer; School of Architecture and Design, Harbin Institute of Technology; Harbin, 150006, China; Key Laboratory of Cold Region Urban and Rural Human Settlement Environment Science and Technology, Ministry of Industry and Information Technology; Harbin, 150090, China; zhibo_zhou@hit.edu.cn



WANG Yan,
Master's Student; School of Architecture and Design, Harbin Institute of Technology; Harbin, 150006, China; Key Laboratory of Cold Region Urban and Rural Human Settlement Environment Science and Technology, Ministry of Industry and Information Technology; Harbin, 150090, China; suncheng@hit.edu.cn



XU Jiawei,
Master; School of Architecture and Design, Harbin Institute of Technology; Harbin, 150006, China; Key Laboratory of Cold Region Urban and Rural Human Settlement Environment Science and Technology, Ministry of Industry and Information Technology; Harbin, 150090, China; suncheng@hit.edu.cn



LI Bo,
Master's Student; School of Architecture and Design, Harbin Institute of Technology; Harbin, 150006, China; Key Laboratory of Cold Region Urban and Rural Human Settlement Environment Science and Technology, Ministry of Industry and Information Technology; Harbin, 150090, China; suncheng@hit.edu.cn

YU Wenrui
Abramova E.V.



YU Wenrui,
Master's Student; School of Architecture and Design, Harbin Institute of Technology; Harbin, 150006, China; Key Laboratory of Cold Region Urban and Rural Human Settlement Environment Science and Technology, Ministry of Industry and Information Technology; Harbin, 150090, China; suncheng@hit.edu.cn



Abramova Elena Vyacheslavovna,
Doctor of Technical Sciences, Professor; Scientific Research Institute of Building Physics of the Russian Academy of Architecture and Building Sciences; 21 Lokomotivny proezd, Moscow, 127238, Russian Federation; Bauman Moscow State Technical University; 2 5 Baumanskaya st., Moscow, 105005, Russian Federation, e.v.abramova11@yandex.ru

neural networks) for machine learning-assisted optimization of long-term hygrothermal performance predictions [9, 10].

Despite these advancements, existing testing methods often require high-end instruments and platforms, resulting in elevated costs that hinder large-scale daily experimentation. Therefore, this study improves upon the traditional cup method by systematically testing three typical building materials — rock wool board, XPS board, and foam concrete — under controlled variables. The results demonstrate that the new scheme not only qualitatively and quantitatively measures water vapour transmission but also enables real-time monitoring of 2D heat and moisture transfer dynamics via embedded sensors, offering a cost-effective and practical solution for fundamental research.

EXPERIMENTAL DESIGN

Materials

1. Rock wool board.

Thermal conductivity of 0.035–0.045 W/m·K, a thermal insulation material formed by high-temperature melting and spinning of natural rocks. It exhibits strong water absorption but maintains long-term weather resistance and stability with proper waterproofing.

2. Foam concrete.

Thermal conductivity of 0.12–0.18 W/m·K, a lightweight insulation material made from cement, quartz sand, and foaming agents. Its porous structure reduces thermal conductivity while allowing vapour transmission to prevent moisture accumulation.

3. Extruded polystyrene (XPS) board.

Thermal conductivity of 0.028–0.035 W/m·K, a rigid foam plastic board with excellent insulation, moisture resistance, and compressive properties.

Methods

1. Experimental Apparatus.

The main components of our experimental setup include a Z-shaped white plastic container, EBS temperature and humidity sensors, an electronic balance accurate to 0.001 g, a black enclosure, a camera recorder, a wax-based sealing compound, and syringes.

The Z-shaped white polyurethane container functions as the primary testing device. It's designed to maintain stable liquid flow and ensure accurate water vapour permeability measurements. At the front, there's a precisely measured 100 × 100 × × 40 mm slot for inserting building material specimens. At the back of the device, there are three evenly spaced circular openings, each 15 mm wide, aligned vertically. This setup divides the interior into four equal parts, making it easier to study how vapour passes through at different heights. The container's bottom holds the liquid that evaporates, while a small 2 mm injection port on the side allows us to carefully add or remove liquid with a syringe. This feature helps control the evaporation process precisely. Overall, this design gives us better management of liquid input and makes the device more reusable.

To keep everything stable during tests, the Z-shaped component is made from lightweight, waterproof, and corrosion-resistant materials, produced through 3D printing. It seals tightly to prevent vapour leaks and remains effective even after long periods of use, helping shield the setup from external environmental factors. Both the top opening and the liquid reservoir feature an equal surface area of 10,000 mml, providing a sufficient evaporation surface and helping to minimize measurement errors caused by inadequate evaporation areas. The structural layout of the apparatus is depicted in Fig. 1.

During the process of installing specimens, to ensure the data are accurate and reliable, all specimens must be fully embedded into the standardized front opening of the apparatus following the specified procedure strictly, and the dimensional deviation of the specimen edges must be controlled within ±3 mm. This is because warping, shrinking, or protrusions could alter the water vapour transmission pathway and lead to measurement inaccuracies.

Before testing, all building material specimens must undergo a drying process to remove free water from their surfaces and interiors, ensuring the validity of subsequent vapour transmission measurements. Once the specimens are dry, gently place them into the front slot of the apparatus. Make sure to seal any gaps completely using a wax-based sealing compound. It's important that the sealing material is waterproof and remains stable over time, without affecting how moisture moves inside the material or disrupting the vapour pressure balance nearby.

Choosing and applying the right sealing agent carefully is essential because using the wrong method could lead to errors in the experiment and result in inaccurate findings. The installation configuration of the specimen is shown in Fig. 2.

2. Assembly and Procedure.

During the experiment, the BES temperature and humidity sensors are first connected to a computer, with the appropriate measurement intervals and sampling frequencies configured to ensure accurate and continuous data acquisition. To ensure the reliability of the measurements, three identical BES sensors are inserted into the three circular probe ports located on the rear of the apparatus. During installation, the front end of each sensor must make full contact with the inner surface of the building material to accurately monitor the dynamic changes in temperature and humidity at the moisture-exposed side. The diameter of each probe hole is matched to the sensor dimensions to ensure a secure fit and minimize measurement errors caused by poor contact.

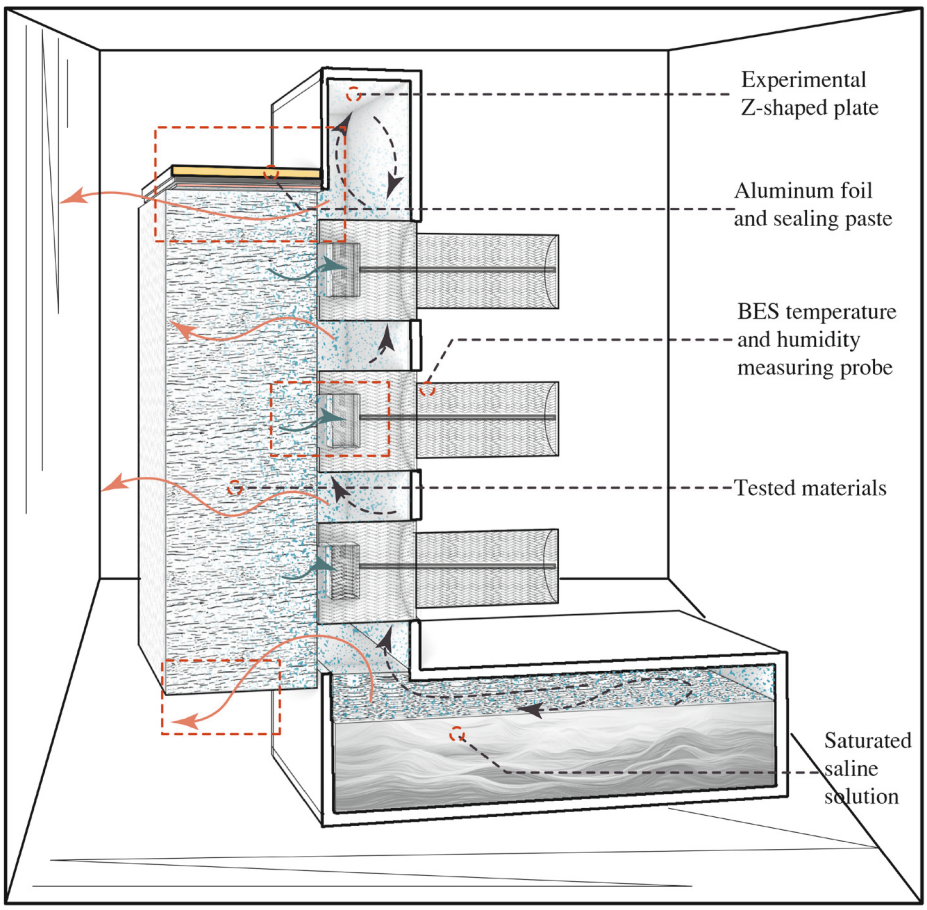


Fig. 1. Structural diagram of the experimental apparatus

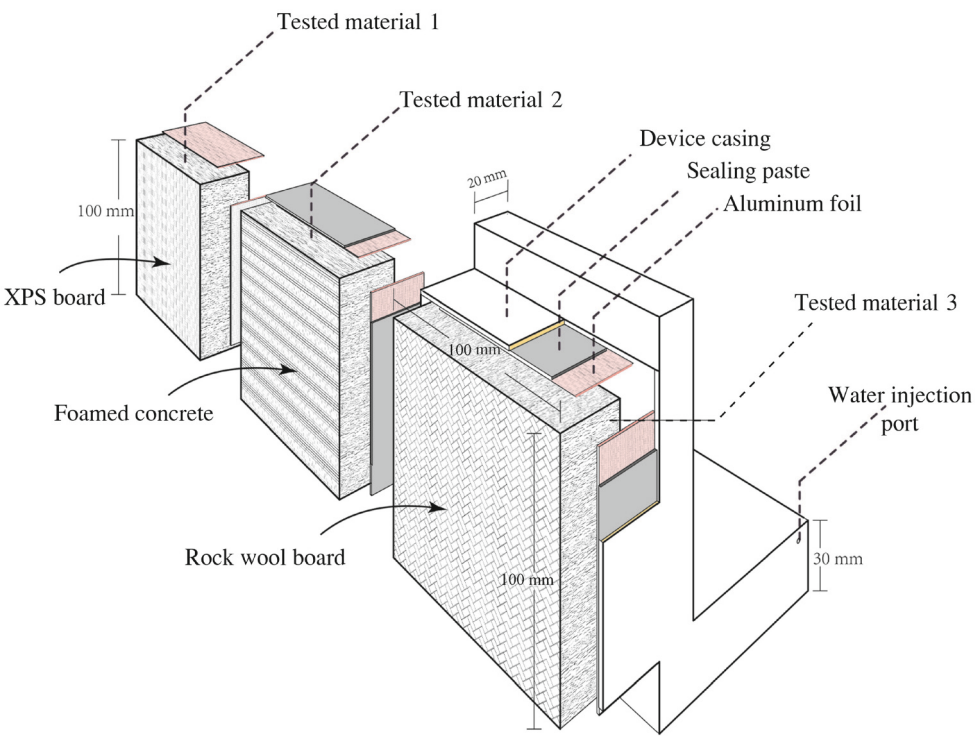


Fig. 2. Illustration of specimen installation

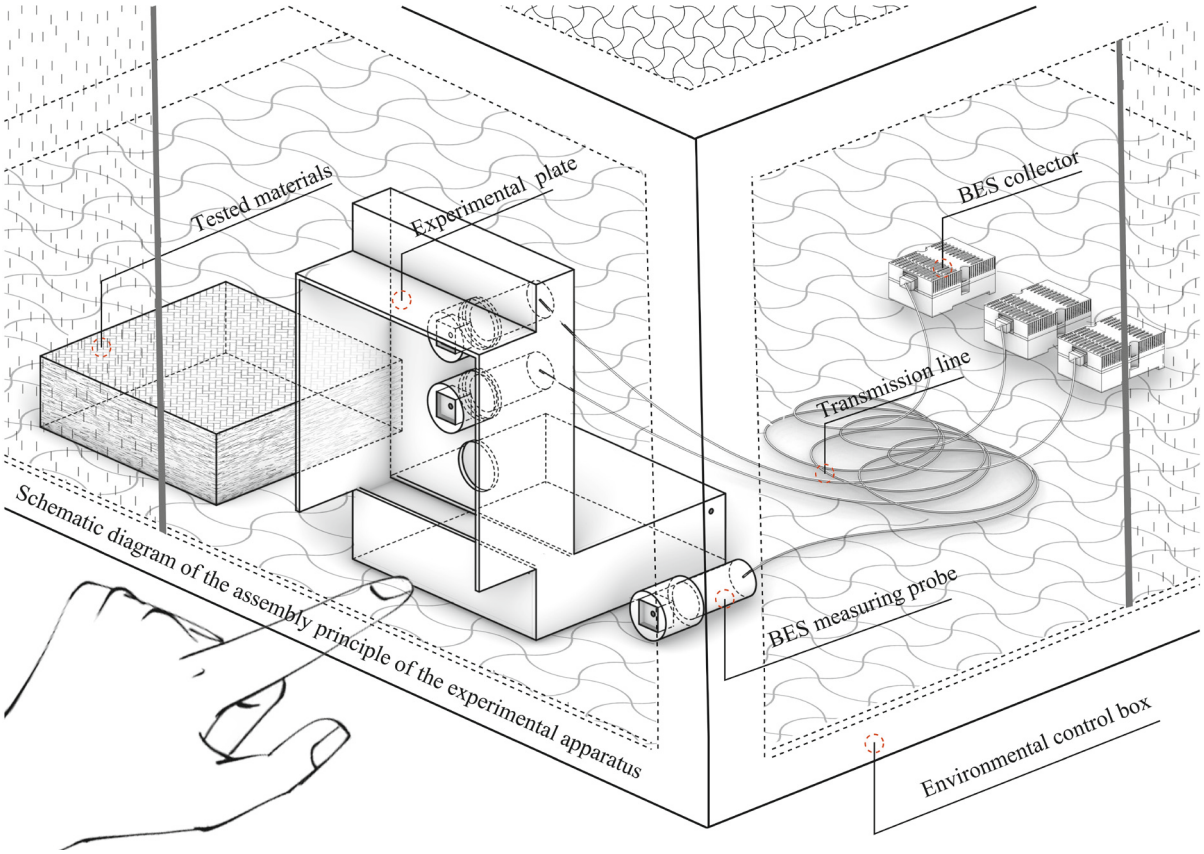


Fig. 3. Schematic diagram of specimen setup and environmental control system

After the building materials are installed, a syringe is used to extract a fixed volume of saturated salt solution, which is slowly injected through the side injection port of the apparatus. The injection process should be carefully controlled in terms of flow rate, and the syringe should be held at a 45° angle to prevent splashing and contamination of the specimen surface. Once the solution is injected, the port is sealed with waterproof adhesive to ensure a stable and airtight test environment inside the apparatus. At this point, the assembly of the core measurement device is complete, providing a reliable foundation for subsequent testing.

For the external testing system, an analytical balance with 1000-g capacity and 0.001-g accuracy is calibrated and zeroed using standard weights. The fully assembled apparatus is then placed centrally and steadily on the weighing platform. Once stabilized, the power is turned on to enable real-time monitoring of mass changes in the Z-shaped apparatus, allowing for precise tracking of transient mass variations.

After assembling the entire system, the setup, which includes the primary testing unit and BES monitoring components, is placed inside an environmental control black box, as shown in the figure. The black box provides a stable ambient environment, where both temperature and relative humidity variations are precisely monitored, providing a comprehensive basis for subsequent data analysis. The principle of specimen setup and system configuration is illustrated in Fig. 3.

This test method is applicable to various types of multi-layer porous building materials and composite wall specimens. When the specimen mass exceeds the standard capacity, counterbalancing weights should be added to the apparatus and an electronic balance with appropriate weighing range must be selected. For specimens exceeding 40 mm in thickness, the front-end structure of the Z-type apparatus should be extended to accommodate dimensional variations. The testing procedure controls humidity conditions on both sides of the specimen to establish water vapour transmission along the path from the high-humidity side to the low-humidity side, thereby obtaining measurements of the material's water vapour permeability characteristics.

ROCK WOOL MATERIAL OBSERVATION TEST

The experiment involved continuous monitoring of water evaporation from rock wool materials. Over a period of 400 hours, periodic measurements were conducted to capture the complete evaporation cycle. In the initial phase, the internal humidity increased rapidly from approximately 10 to 45 %, followed by fluctuations, indicating an unstable equilibrium. During this stage, a dynamic balance was observed between water evaporation from the solution and moisture diffusion from the material surface, suggesting a steady evaporation process.

After approximately 200 hours, as the majority of the water had evaporated, the surface humidity exhibited more pronounced fluctuations, reflecting the transition to a drying-dominated phase. Following about 15 hours of high-amplitude oscillations, the relative humidity decreased rapidly and gradually converged with the ambient humidity level, marking the completion of the first full evaporation cycle in the rock wool material. The data acquisition and monitoring process are illustrated in Fig. 4.

1. Experimental results analysis.

Based on the dynamic characteristics of relative humidity changes on the moisture-exposed surface during water vapour

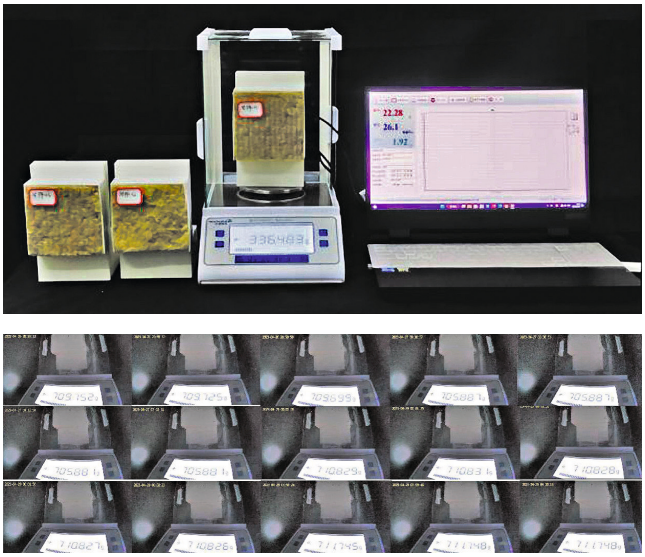


Fig. 4. Schematic diagram of the experimental setup for rock wool evaporation monitoring

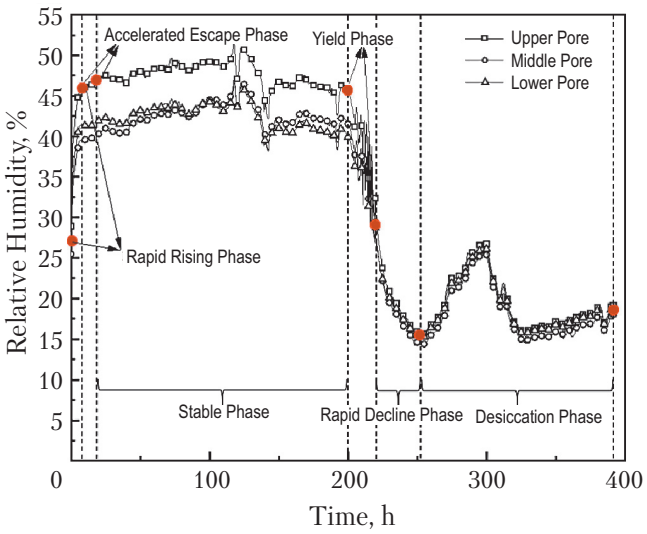


Fig. 5. Rock Wool Moisture-Exposed Surface Humidity Variation Curve

evaporation, the evaporation cycle was divided into six typical stages: rapid rising phase, accelerated escape phase, stable phase, yield phase, rapid decline phase, and dry phase. This staging method helps systematically analyze the water vapour penetration mechanism in building porous materials. In addition, comparative analysis of relative humidity changes at three monitoring points (upper, middle, and lower) on the moisture-exposed surface of porous materials revealed that the upper point maintained the highest relative humidity, averaging about 5 % higher than the middle and lower points during the stable phase. In the initial test stage, the lower point showed slightly higher relative humidity than the middle point, but as the test progressed, the middle point gradually surpassed the lower point, with both exhibiting an alternating upward trend.

Notably, when the solution was nearly evaporated, all monitoring points experienced significant high-amplitude fluctuations before eventually converging to similar humidity levels, as shown in Fig. 5.

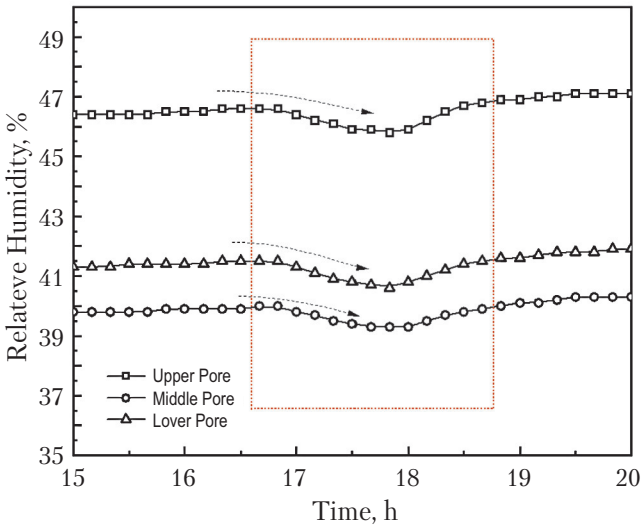


Fig. 6. Detailed view of the accelerated escape phase in rock wool testing

During the monitoring of the accelerated escape phase at the moisture-exposed surface of rock wool, the relative humidity (RH) rapidly decreased by approximately 2 % within 60 min from a previously stable state. Notably, this transient characteristic was also observed in tests involving foam concrete and extruded polystyrene (XPS) boards. However, due to differences in material permeability, the duration of the accelerated escape phase varied among these materials, as illustrated in Fig. 6.

Through continuous 15-hour observation of the yield phase in rock wool's moisture-exposed surface humidity variation, experimental data revealed significant periodic fluctuations in relative humidity (RH), with peak-to-trough differences of 5–10 %. Throughout the monitoring period, the RH curve exhibited an overall decreasing trend. The three detection points (upper, middle, and lower) on the moisture-exposed surface showed highly consistent RH variations while maintaining distinct vertical gradients: the upper point consistently recorded the highest RH, followed by the middle and then the lower point. Quantitative analysis demonstrated that the absolute RH difference between the upper and middle points persistently exceeded that between the middle and lower points.

Toward the end of the yield phase, the RH curves from all three points gradually converged. Correlated with electronic balance measurements and solution replenishment mass analysis, the yield phase was identified as corresponding to the final stage of solution evaporation. During this phase, decreased evaporation rates caused reduced water vapour partial pressure within the apparatus, triggering the observed periodic RH fluctuations at rock wool's moisture-exposed surface, as detailed in Fig. 7.

2. Supplementary test analysis.

This study systematically analyzed the water vapour permeability characteristics of rock wool by comparing its performance changes after experiencing a complete evaporation cycle. After refilling the evaporated apparatus with saturated salt solution, performance comparison tests were conducted under identical environmental conditions. Comparative analysis of temperature and humidity change curves at the moisture-exposed surface of rock wool in both dry and wet states revealed that the entire humidity variation process could still be divided into six typical stages, although significant data fluctuations were observed during

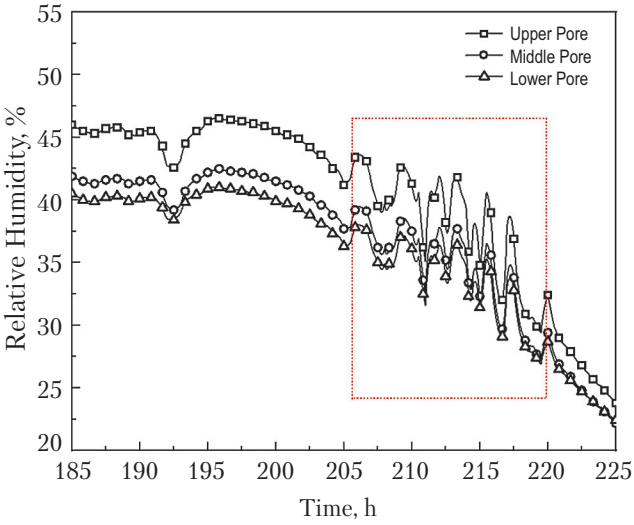


Fig. 7. Detailed view of the yield phase in rock wool testing

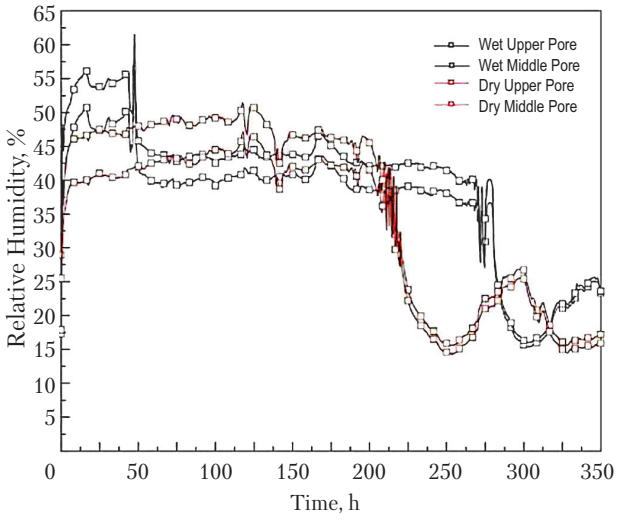


Fig. 8. Detailed view of the yield phase in rock wool testing

the stable phase. Experimental data showed that due to the increased mass of saturated solution, the duration of stable evaporation phase was significantly prolonged.

Specifically, during the rapid rising phase of relative humidity, the internal surface humidity of wet-state rock wool panels was higher than that of dry-state specimens, with more pronounced fluctuation amplitudes during the accelerated escape phase. After undergoing a yield phase similar to the dry state, the wet-state specimens entered a comparable drying phase with minimal humidity value differences, as shown in Fig. 8.

Analysis indicates that after undergoing a complete evaporation cycle, the rock wool material exhibits significantly different drying characteristics compared to its initial state. The reduced moisture gradient within the material slows down water vapour diffusion to some extent, decreasing vapour permeability. Consequently, during the rapid rising phase, the relative humidity near the interior surface reaches higher values than previously observed. This phenomenon creates an enhanced vapour pressure differential between the apparatus's inner and outer surfaces, leading to more vigorous vapour dissipation during the accelerated escape phase. Following this intensified dissipation, the system enters a stabilization period with fluctuations similar in magnitude to the dry-state condition, albeit within a narrower range.

Experimental results demonstrate that after completing a full evaporation cycle, the primary effect observed in rock wool panels — whether in dried or re-wetted conditions — is altered vapour accumulation characteristics during the initial phase, with no significant material performance degradation detected. Regarding the pronounced curve fluctuations during the stabilization phase, these anomalies may potentially stem from instrumentation measurement errors, though current evidence remains insufficient to establish definitive theoretical explanations.

Due to the relatively low overall evaporation rate of the materials — particularly the significantly prolonged evaporation cycles observed in materials with higher vapour permeation resistance — this study was unable to conduct complete evaporation cycle observations for foam concrete and extruded polystyrene (XPS) boards within the experimental timeframe. The investigation was limited to recording the relative humidity variation process from the rapid rising phase through the stabilization phase. Experimental results are presented in Fig. 9–12.

Under identical saturated solution mass injection conditions, foam concrete and extruded polystyrene (XPS) boards exhibited significantly prolonged evaporation cycles compared to rock wool. The moisture-exposed surfaces of these materials maintained higher relative humidity levels: foam concrete showed a gradual decline from an initial 85 % high, while XPS boards sustained persistent high-level fluctuations without observable decreasing trends. In contrast, rock wool completed its entire evaporation cycle within 300 hours, demonstrating approximately 35 % lower relative humidity during the stable evaporation phase than the other two building materials. These observations align with the anticipated water vapour permeability characteristics of the three materials, as illustrated in Fig. 13.

Experimental results of water vapour permeation rates generally corresponded with theoretical predictions. Rock wool displayed superior vapour permeability, whereas XPS boards — due to their lower evaporation rates — produced data with greater fluctuations that somewhat compromised measurement reliability. Nevertheless, the obtained water vapour transmission rates effectively

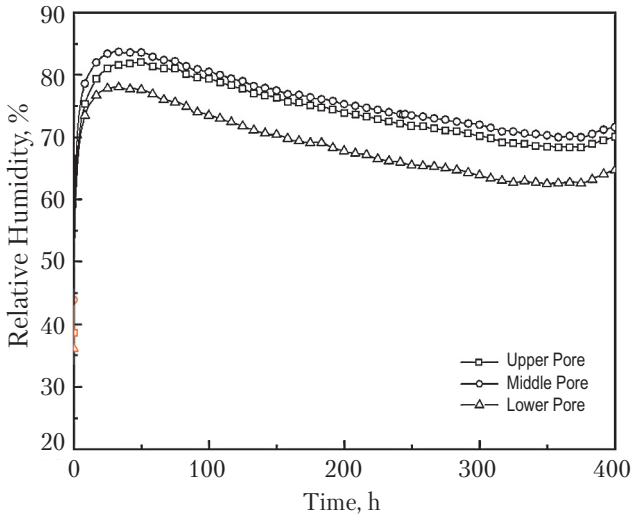


Fig. 9. Humidity variation curve at the moisture-exposed surface of foam concrete

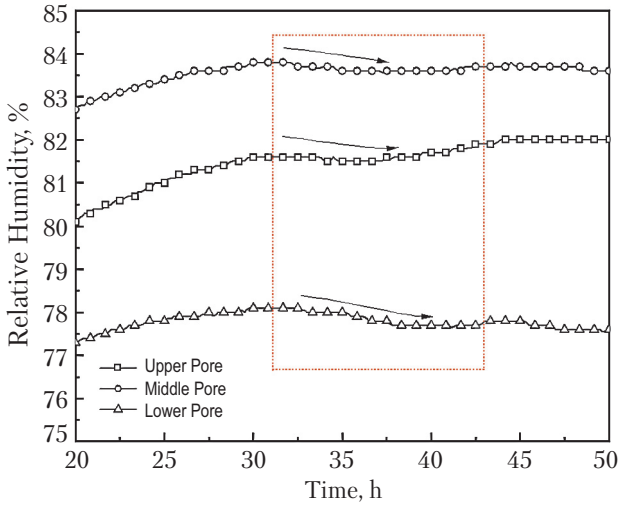


Fig. 10. Detailed view of the accelerated escape phase in foam concrete testing

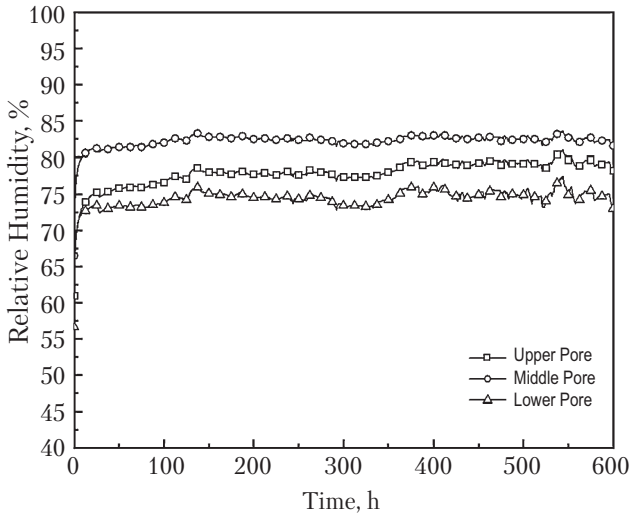


Fig. 11. Humidity variation curve at the moisture-exposed surface of XPS board

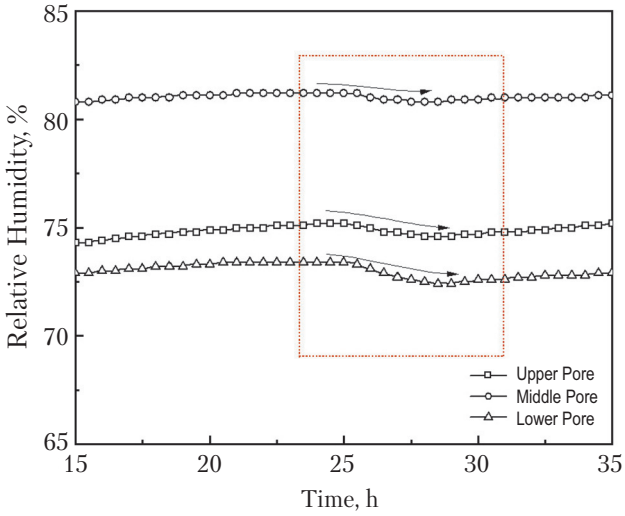


Fig. 12. Detailed view of the accelerated escape phase in XPS board testing

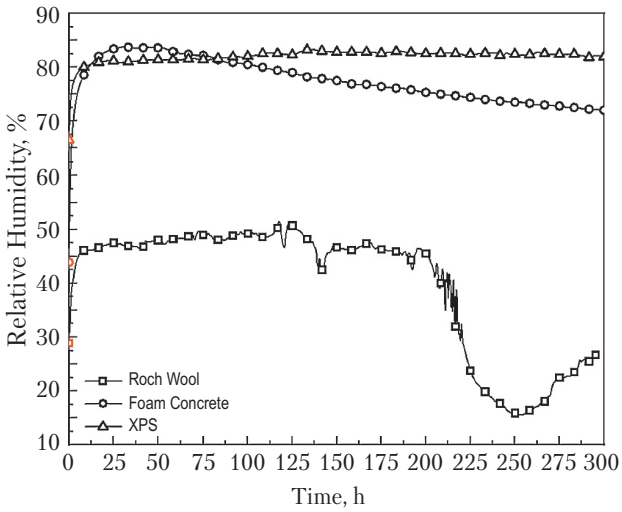


Fig. 13. Comparative analysis of humidity variation curves across materials

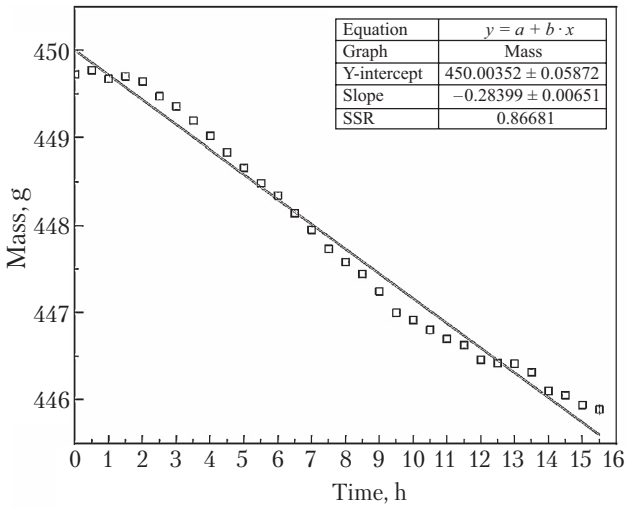


Fig. 14. Water vapour permeability fitting curve for rock wool board

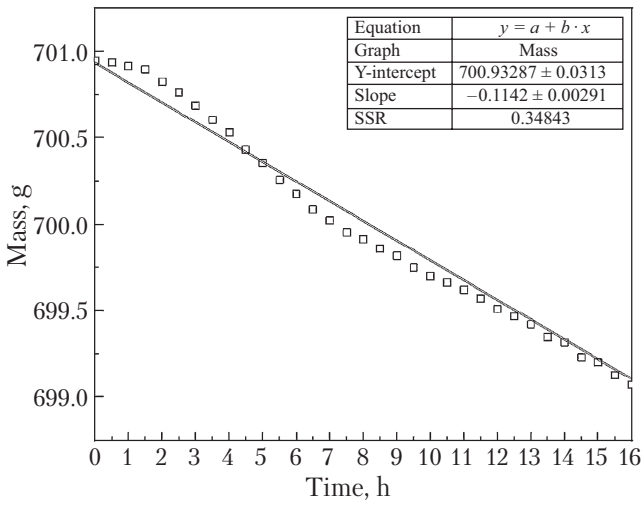


Fig. 15. Water vapour permeability fitting curve for foam concrete

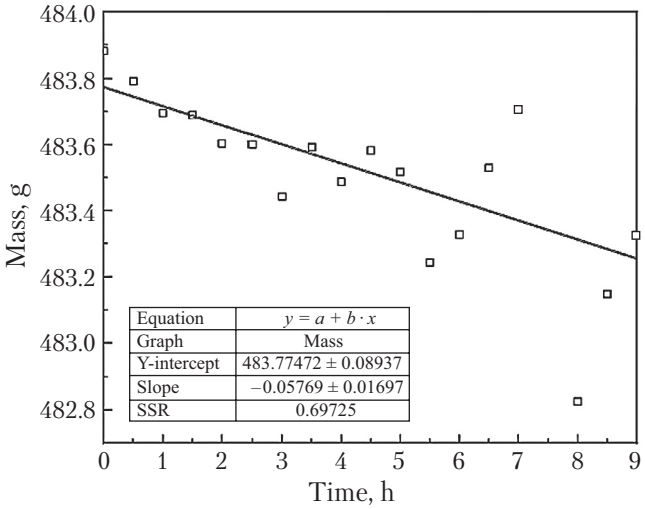


Fig. 16. Water vapour permeability fitting curve for XPS board

represent each material's intrinsic properties. Quantitative permeability results are presented in Fig. 14–16.

CONCLUSION

This study investigated rock wool boards, extruded polystyrene (XPS) panels, and foam concrete through an improved two-dimensional heat-moisture transfer experimental protocol, revealing dynamic hygrothermal migration patterns in porous building materials. The experiments demonstrated that material vapour permeability significantly influences evaporation cycles and humidity distribution: foam concrete and XPS panels exhibited prolonged evaporation cycles with moisture-exposed surface relative humidity maintained at 85 % due to their high vapour resistance, while rock wool›s loose structure resulted in a shorter 300-hour evaporation cycle with 35 % lower humidity during stabilization, confirming theoretical vapour permeability predictions.

The research further identified an accelerated escape phenomenon occurring when vapour breached the material-environment interface barrier, causing abrupt vapour pressure differential reduction. Distinct humidity distribution patterns were observed: rock wool showed highest humidity at upper monitoring points due to unsealed bottom edges, whereas foam concrete and XPS panels exhibited mid-point and upper-mid-point dominance respectively, reflecting their dense structures› impact on vapour pathways. These findings provide empirical evidence for building envelope sealing design.

The experimental protocol achieved dynamic 2D monitoring through embedded sensors, balancing cost-efficiency with operability. However, time constraints limited complete evaporation mechanism analysis for high-resistance materials, warranting longer-term observation. Future studies could integrate numerical modeling or micro-imaging to examine pore structure and interface effects on coupled heat-moisture transfer. These results establish both theoretical and practical foundations for optimizing energy-efficient materials and hygrothermal environment control.

REFERENCES

1. Balaji N.C., Mani M., Reddy B.V.V. Discerning Heat Transfer in Building Materials. Energy Procedia. 2014; 54:654-668.
2. Lei Y., Yang H., Zhang Y. et al. Review of test methods and current status of hygrothermal physical properties of porous building materials. Building Science. 2021; 37(2):165-173+184. DOI: 10.13614/j.cnki.11-1962/tu.2021.02.23
3. Feng C., Zhong H., Feng Y. et al. Advances in testing hygric properties of porous building materials. Proceedings of the 12th National Conference on Building Physics. 2016; 44-48.
4. Feng C., Yu X., Wang D. Determination of hygric properties of aerated concrete. Journal of Civil, Architectural & Environmental Engineering. 2016; 38(2):125-131.
5. Zeng H., Jin M., Li W. et al. Performance evolution of low heat cement under thermal cycling fatigue: A comparative study with moderate heat cement and ordinary Portland cement. Construction and Building Materials. 2024; 412:134863.
6. He J., Li Q., Meng Q. et al. Experimental study on hygroscopic behaviour of salt-containing aerated concrete. Building Science. 2023; 39(6):10-17. DOI: 10.13614/j.cnki.11-1962/tu.2023.06.02
7. Jin M., Ma Y., Li W. et al. Multi-scale investigation on composition-structure of C-(A)-S-H with different Al/Si ratios under attack of decalcification action. Cement and Concrete Research. 2023; 172:107251.
8. Guimarães A.S., Ribeiro I.M., Freitas T.S. TRHUMIDADE — A water diffusivity model to predict moisture content profiles. Cogent Engineering. 2018; 5(1):1459007.
9. Yin X., Li X., Huang Z. et al. Prediction of concrete hydration heat temperature by integrating digital twin and LSTM neural network. Journal of Xi'an University of Architecture & Technology (Natural Science Edition). 2025; 57(2):167-173+316. DOI: 10.15986/j.1006-7930.2025.02.002
10. Yang G., Ye T., Wang G. Prediction analysis of foundation pit deformation based on genetic algorithm optimized LSTM neural network. Anhui Architecture. 2025; 32(4):116-118+176. DOI: 10.16330/j.cnki.1007-7359.2025.4.35

Предварительная экспериментальная схема двумерного тепло- и влагопереноса в строительных пористых материалах

Для исследования двумерного процесса тепло- и влагопереноса в строительных пористых материалах и анализа влияния условий уплотнения кромок на их теплофизические и гигроскопические свойства в данном исследовании предлагается новая экспериментальная схема. В качестве образцов для испытаний были выбраны три типичных строительных материала — плита из минеральной ваты, экструдированный полистирол (ЭППС) и пенобетон. С помощью мониторинга изменений температуры и влажности в режиме реального времени внутри и снаружи экспериментальной установки были изучены взаимосвязанные характеристики тепло- и влагопередачи различных материалов. Результаты показывают, что материалы с высокой паропроницаемостью и эффективной воздухонепроницаемостью значительно повышают термическую и гигроскопическую стабильность. Кроме того, в пористых материалах со слабой структурой потеря влаги через боковые кромки приводит к неравномерному распределению влажности внутри материала. Основываясь на экспериментальных данных, в этом исследовании были количественно определены коэффициенты паропроницаемости трех материалов и выяснены лежащие в их основе механизмы. Предлагаемый экспериментальный метод устанавливает новый подход к измерению двумерного сопряженного тепло- и влагопереноса в строительных материалах, обеспечивая научную основу для изучения механизмов переноса тепла и влаги в архитектурных приложениях.

Ключевые слова: *пористые материалы, тепло-влагоперенос, протокол эксперимента*

СПИСОК ИСТОЧНИКОВ

1. Balaji N.C., Mani M., Reddy B.V.V. Discerning Heat Transfer in Building Materials // Energy Procedia. 2014. No. 54. Pp. 654–668.
2. Lei Y., Yang H., Zhang Y. et al. Review of test methods and current status of hygrothermal physical properties of porous building materials // Building Scienc. 2021. No. 37 (2). Pp. 165–173+184. DOI: 10.13614/j.cnki.11-1962/tu.2021.02.23
3. Feng C., Zhong H., Feng Y. et al. Advances in testing hygric properties of porous building materials // Proceedings of the 12th National Conference on Building Physics. 2016. Pp. 44–48.
4. Feng C., Yu X., Wang D. Determination of hygric properties of aerated concrete // Journal of Civil, Architectural & Environmental Engineering. 2016. No. 38 (2). Pp. 125–131.
5. Zeng H., Jin M., Li W. et al. Performance evolution of low heat cement under thermal cycling fatigue: A comparative study with moderate heat cement and ordinary Portland cement // Construction and Building Materials. 2024. No. 412. P. 134863.
6. He J., Li Q., Meng Q. et al. Experimental study on hygroscopic behaviour of salt-containing aerated concrete // Building Science. 2023. No. 39 (6). Pp. 10–17. DOI: 10.13614/j.cnki.11-1962/tu.2023.06.02
7. Jin M., Ma Y., Li W. et al. Multi-scale investigation on composition-structure of C-(A)-S-H with different Al/Si ratios under attack of decalcification action // Cement and Concrete Research. 2023. No. 172. P. 107251.
8. Guimar es A.S., Ribeiro I.M., Freitas T.S. TRHUMIDADE — A water diffusivity model to predict moisture content profiles // Cogent Engineering. 2018. No. 5 (1). P. 1459007.
9. Yin X., Li X., Huang Z. et al. Prediction of concrete hydration heat temperature by integrating digital twin and LSTM neural network // Journal of Xi'an University of Architecture & Technology (Natural Science Edition). 2025. No. 57 (2). Pp. 167–173+316. DOI: 10.15986/j.1006-7930.2025.02.002
10. Yang G., Ye T., Wang G. Prediction analysis of foundation pit deformation based on genetic algorithm optimized LSTM neural network // Anhui Architecture. 2025. No. 32 (4). Pp. 116-118+176. DOI: 10.16330/j.cnki.1007-7359.2025.4.35

Об авторах: **Джоу Джибо** — кандидат наук, преподаватель; **Школа архитектуры и дизайна, Харбинский технологический институт**; 150006, г. Харбин, Китай; **Ключевая лаборатория науки и технологий в области окружающей среды городских и сельских населенных пунктов Холодного региона, Министерство промышленности и информационных технологий**; 150006, г. Харбин, Китай; zhibo_zhou@hit.edu.cn;

Ван Янь — магистрант; **Школа архитектуры и дизайна, Харбинский технологический институт**; 150006, г. Харбин, Китай; **Ключевая лаборатория науки и технологий в области окружающей среды городских и сельских населенных пунктов Холодного региона, Министерство промышленности и информационных технологий**; 150006, г. Харбин, Китай; suncheng@hit.edu.cn;

Сюй Цзявэй — магистр; **Школа архитектуры и дизайна, Харбинский технологический институт**; 150006, г. Харбин, Китай; **Ключевая лаборатория науки и технологий в области окружающей среды городских и сельских населенных пунктов Холодного региона, Министерство промышленности и информационных технологий**; 150006, г. Харбин, Китай; suncheng@hit.edu.cn;

Ли Бо — магистрант; **Школа архитектуры и дизайна, Харбинский технологический институт**; 150006, г. Харбин, Китай; **Ключевая лаборатория науки и технологий в области окружающей среды городских и сельских населенных пунктов Холодного региона, Министерство промышленности и информационных технологий**; 150006, г. Харбин, Китай; suncheng@hit.edu.cn;

Юй Вэньруй — магистрант; **Школа архитектуры и дизайна, Харбинский технологический институт**; 150006, г. Харбин, Китай; **Ключевая лаборатория науки и технологий в области окружающей среды городских и сельских населенных пунктов Холодного региона, Министерство промышленности и информационных технологий**; 150006, г. Харбин, Китай; suncheng@hit.edu.cn;

Абрамова Елена Вячеславовна — д-р техн. наук, профессор; **Научно-исследовательский институт строительной физики Российской академии архитектуры и строительных наук**; 127238, г. Москва, Локомотивный проезд, д. 21, Российская Федерация; **Московский государственный технический университет имени Н.Э. Баумана**; г. Москва, ул. Бауманская, д. 2, стр. 5, 105005; e.v.abramova11@yandex.ru.

For citation: ZHOU Zhibo, WANG Yan, XU Jiawei, LI Bo, YU Wenrui, Abramova E.V. Preliminary experimental scheme for two-dimensional heat and moisture transfer in porous building materials. *Real Estate: Economics, Management*. 2025; 3:53-61.

Для цитирования: *Джоу Джибо, Ван Янь, Сюй Цзявэй, Ли Бо, Юй Вэньруй, Абрамова Е.В.* Preliminary experimental scheme for two-dimensional heat and moisture transfer in porous building materials // Недвижимость: экономика, управление. 2025. № 3. С. 53–61.